iScience

CellPress
OPEN ACCESS

Article

Androgen-regulated *MafB* drives cell migration via MMP11-dependent extracellular matrix remodeling in mice

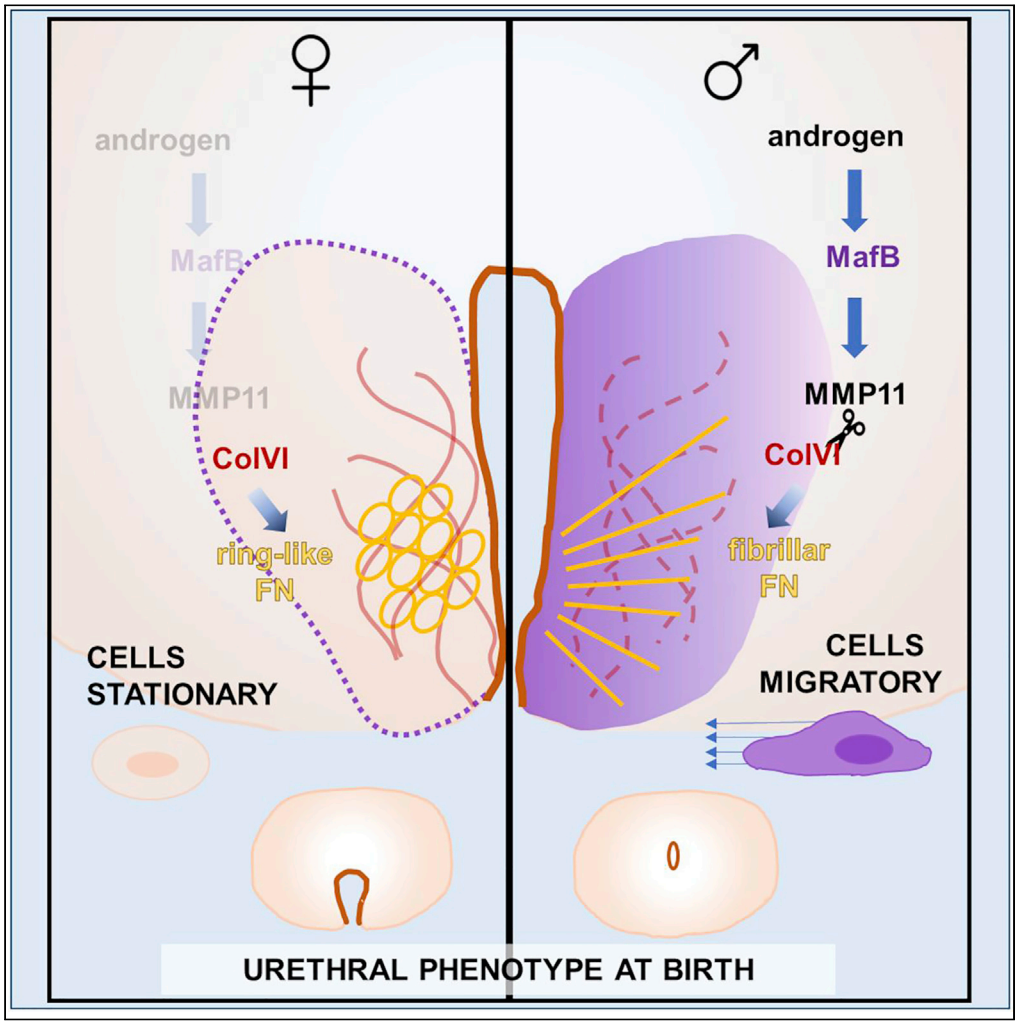

Mellissa C. Alcantara, Kentaro Suzuki, Alvin R. Acebedo, ..., Kazuo Yamagata, Satoru Takahashi, Gen Yamada

k-suzuki@wakayama-med.ac.jp (K.S.)
genyama@yahoo.co.jp (G.Y.)

Highlights

Androgen-regulated *MafB* is required for cell migration in urethral masculinization

MafB upregulates *Mmp11* during urethral masculinization

MMP11 cleaves CollagenVI, resulting in fibrillar fibronectin deposition

MafB-expressing mesenchymal cells migrate on fibronectin, but not on CollagenVI

Alcantara et al., iScience *25*, 105609
December 22, 2022 © 2022
https://doi.org/10.1016/j.isci.2022.105609

iScience

CellPress
OPEN ACCESS

Article

Androgen-regulated *MafB* drives cell migration via MMP11-dependent extracellular matrix remodeling in mice

Mellissa C. Alcantara,[1] Kentaro Suzuki,[1,*] Alvin R. Acebedo,[1] Daiki Kajioka,[1] Satoshi Hirohata,[2] Tsuneyasu Kaisho,[3] Yu Hatano,[4] Kazuo Yamagata,[4] Satoru Takahashi,[5] and Gen Yamada[1,6,*]

SUMMARY

While androgen is considered a pivotal regulator of sexually dimorphic development, it remains unclear how it orchestrates the differentiation of reproductive organs. Using external genitalia development as a model, we showed that androgen, through the transcription factor *MafB*, induced cell migration by remodeling the local extracellular matrix (ECM), leading to increased cell contractility and focal adhesion assembly. Furthermore, we identified the matrix metalloproteinase *Mmp11* as a *MafB* target gene under androgen signaling. MMP11 remodels the local ECM environment by degrading Collagen VI (ColVI). The reduction of ColVI led to the fibrillar deposition of fibronectin in the *MafB*-expressing bilateral mesenchyme both *in vivo* and *ex vivo*. The ECM remodeling and development of migratory cell characteristics were lost in the *MafB* loss-of-function mice. These results demonstrate the requirement of mesenchymal-derived androgen signaling on ECM-dependent cell migration, providing insights into the regulatory cellular mechanisms underlying androgen-driven sexual differentiation.

INTRODUCTION

Androgen is the key regulator for the sexually dimorphic development of the external genitalia.[1] Arising from a common anlage, the male and female embryonic external genitalia (eExG) of mice begin to show sexual differences at embryonic day (E) 15.5. Under androgen regulation, the urethra of male mice canalizes around E16.5, a process termed urethral masculinization. In contrast, the ventral side of the urethra remains open in females. V-maf avian musculoaponeurotic fibrosarcoma oncogene homolog B (*MafB*) is a transcription factor that is expressed in the mesenchyme lateral to the presumptive urethra, hereafter referred to as the bilateral mesenchyme (biMs). Previously, *MafB* has been identified to be a direct androgen target that is essential for urethral masculinization: male *MafB* mutant mice show an abnormal, open urethra.[2,3] Prior to androgen induction, *MafB* is required for vascular differentiation during testicular organogenesis (Li et al., 2021). Although several androgen-regulated cellular processes during urethral masculinization have been described,[1,4–8] how *MafB* contributes to this event has yet to be defined.

During organogenesis, androgens have been reported to regulate the cytoskeletal elements during urethral masculinization.[4,5] In this study, we observed defects in cell migration in the *MafB* knockout mice; therefore, a unique pathway is likely downstream of androgen-MafB signaling. Cell migration is highly influenced by either the composition, stiffness, or concentration of the ECM.[9,10] Matrix metalloproteinases (MMPs) are endopeptidases that can cleave matrix proteins and remodel the ECM environment. Their function is essential for both developmental and pathological processes, especially in cancer.[11] MMP11, also known as stromelysin-3, is an MMP that was first isolated from breast cancer tissue.[12,13] During embryogenesis, *Mmp11* is expressed transiently in mesenchymal cells that are associated with tissue remodeling[14–16]; however, in healthy adult human organs, *Mmp11* is seldom expressed.[17]

MMP11 has been reported to cleave the α3 subunit of ColVI,[18] a ubiquitous ECM protein that interacts with other ECM proteins to form a structural network for cells.[19] One such interaction is with the ECM protein fibronectin (FN), wherein ColVI expression regulates the deposition pattern of FN.[20–22] FN participates in cell differentiation, growth factor signaling, and cell migration.[23] In several biological systems,

[1]Department of Developmental Genetics, Institute of Advanced Medicine, Wakayama Medical University, Wakayama 641-8509, Japan

[2]Department of Medical Technology, Graduate School of Health Sciences, Okayama University, 2-5-1 Shikata-cho, Kita-ku, Okayama 700-8558 Japan

[3]Department of Immunology, Institute of Advanced Medicine, Wakayama Medical University, Kimiidera, Wakayama 641-8509, Japan

[4]Faculty of Biology-Oriented Science and Technology, Kindai University, Kinokawa-shi, Wakayama 649-6493, Japan

[5]Department of Anatomy and Embryology, Laboratory Animal Resource Center in Transborder Medical Research Center, Faculty of Medicine, University of Tsukuba, Tennodai, Tsukuba, Ibaraki 305, Japan

[6]Lead contact

*Correspondence: k-suzuki@wakayama-med.ac.jp (K.S.), genyama@yahoo.co.jp (G.Y.)

https://doi.org/10.1016/j.isci.2022.105609

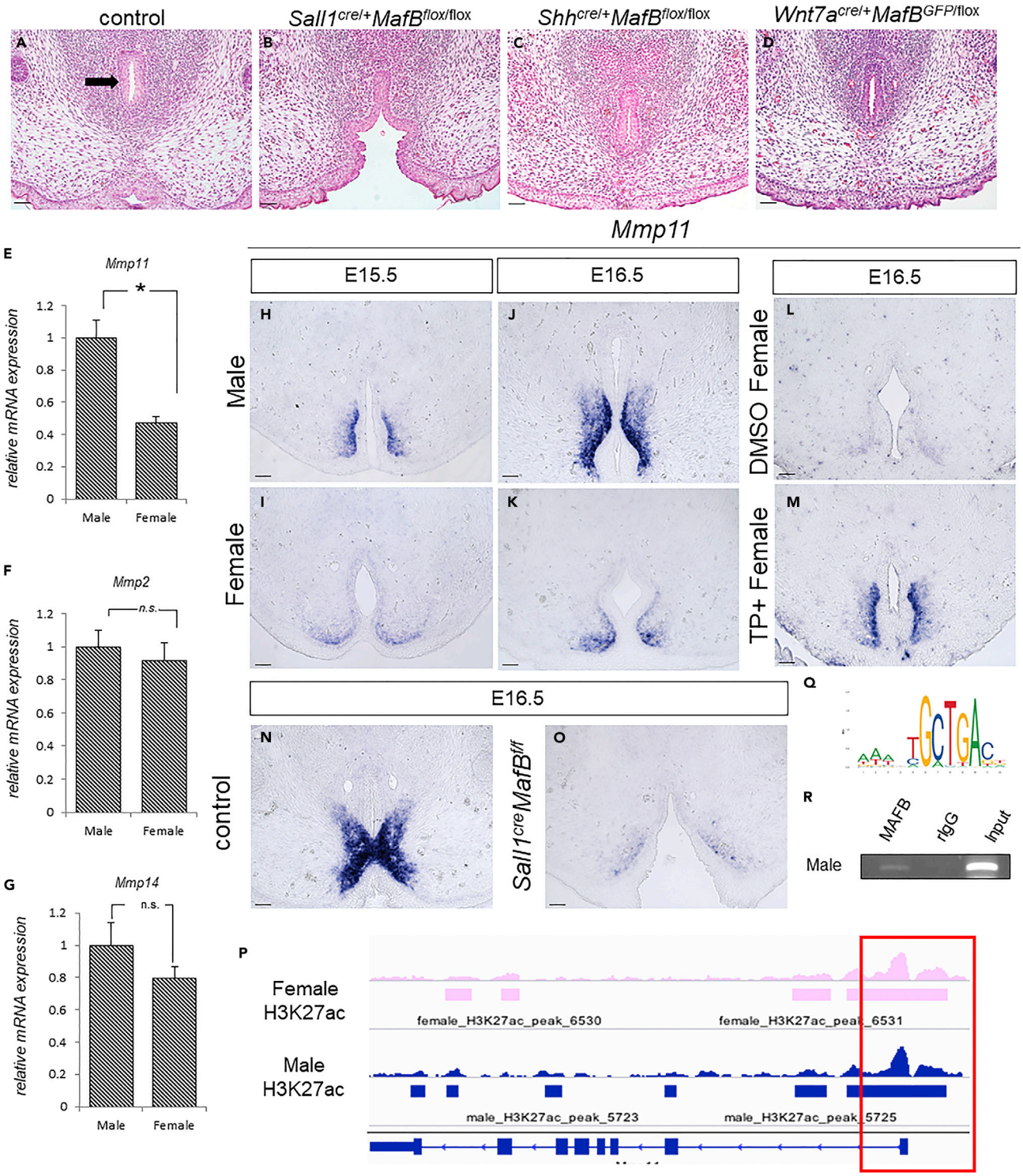

Figure 1. Mesenchymal *MafB* regulates *Mmp11* during urethral masculinization

[A–D] Mesenchymal, not epithelial, *MafB* is involved in urethral masculinization. See also Figure S1A. (A) The formation of a urethral tube (arrow) was observed in E16.5 control mice. (B) Mesenchymal-specific *MafB* knockout mice ($Sall1^{cre/+};MafB^{flox/flox}$) failed to form a urethral tube. (C) Endodermal epithelium-specific *MafB* knockout mice ($Shh^{cre/+};MafB^{flox/flox}$) exhibited a masculinized urethral tube. (D) Ectodermal epithelium-specific *MafB* knockout mice ($Wnt7a^{cre/+};MafB^{GFP/flox}$) exhibited a masculinized urethral tube. Scale bar: 50 μm [E-N] *Mmp11* is involved in urethral masculinization. See also Figures S1B and S1C.

Figure 1. *Continued*

(E–G) Gene expression analysis of *Mmp11* (E), *Mmp2* (F), and *Mmp14* (G) revealed that *Mmp11* is sexually dimorphic. Data expressed as mean ± SEM
*p < 0.05, t-test.

(H–K) *Mmp11* was expressed more strongly in the biMs of male mice at E15.5 (H) and E 16.5 (J) compared to the female (I and K). Scale bar: 50 μm. (L and M) *Mmp11* expression was induced with testosterone proprionate (TP) treatment. Scale bar: 50 μm [N–S] *Mmp11* is under *MafB*-regulation. See also Figure S1D.

(N and O) *Mmp11* expression was downregulated in the mesenchymal-specific *MafB* knockout. Scale bar: 50 μm.

(P) An H3K27ac element is present in the *Mmp11* promoter region.

(Q) *MafB*-binding sequence (MARE).

(R) ChIP-PCR analysis confirmed that MAFB was present in the H3k27ac element within the *Mmp11* promoter region.

perturbations in FN expression led to phenotypes associated with impaired cell migration,[24–26] and the fibrillar deposition of FN has also been correlated with cell movement.[27–29] In fact, the FN network continuously changes during embryonic development: In the *Xenopus* embryo, FN fibrils are constantly remodeled from gastrulation until neurulation,[30] while spatiotemporal differences in the pattern of FN deposition accompany palate shelf elevation.[31] Both neurulation and palatogenesis are widely accepted models for the investigation of tissue fusion, which both point to the importance of spatiotemporal regulation of FN during midline fusion in organogenesis.[32,33] Since the male-type urethra also undergoes migration and fusion events, we investigated whether FN was involved in this process.

Here, we elucidate the mechanism of androgen-driven cell migration during male eExG development. We demonstrate MMP11-dependent ECM remodeling during sexual differentiation. MMP11-degradation of ColVI changes the ECM microenvironment and promotes focal adhesion formation and cell contractility. Furthermore, we propose that *MafB* regulates *Mmp11* under androgen signaling and reveal the significance of this signaling cascade during urethral masculinization.

RESULTS

MafB regulates biMs cell migration into the midline

Androgen-driven biMs cell migration is one of the essential processes for the eExG development.[4,5] To understand the role of *MafB* during urethral masculinization, we cultured tissue slices from the eExG of $MafB^{GFP/GFP}$ knockout (*MafB* KO) and control mice for 48 h. Cells of the biMs in the control slices actively migrated toward the midline, forming the urethral tube (Video S1). In contrast, biMs cells of the *MafB* KO, while motile, remained in place (Video S2). These data suggest that *MafB* is necessary for cell migration during urethral masculinization.

Mesenchymal *MafB* function is required for urethral masculinization

Although MAFB is predominantly expressed in the biMs, it is also expressed in the epithelia (Figure S1A). To confirm whether only mesenchymal *MafB* is crucial to urethral masculinization, we analyzed several conditional knockout mice which specifically targeted the mesenchymal, endodermal-epithelial, and ectodermal-epithelial *MafB* in the eExG (Figures 1A-1D). *Sall1* has previously been reported to be expressed in the biMs, while *Shh* (Sonic hedgehog) is specific to the endoderm-derived urethral epithelium.[5] Meanwhile, *Wnt7a* is expressed in the ectodermal epithelium of the eExG.[34] At E16.5, only the mesenchymal $Sall1^{cre/+}MafB^{f/f}$ (*MafB* cKO) mice showed the female-like open urethra, similar to the conventional knockout mice.[3] The urethral tube was formed completely in the other two mutants, indicating that mesenchymal *MafB* is essential for androgen-driven urethral masculinization.

MMP11 is a *MafB*-regulated, sexually dimorphic metalloproteinase in the embryonic external genitalia

We hypothesized that *MafB* drives urethral masculinization through the regulation of cell migration. Modifications in the composition or arrangement of the ECM are known to regulate cell migration,[9] and one of the known mechanisms by which the ECM is remodeled is through MMPs. We performed RNA-seq analysis of the biMs to investigate their transcriptomic expression profile and observed that *Mmp2*, *Mmp11*, and *Mmp14* were the most highly expressed MMPs in the biMs of the eExG at E16.5 (GEO: GSE185966). However, RT-qPCR analysis determined that only *Mmp11* was a sexually dimorphic gene (Figures 1E–1G). Indeed, both MMP11 mRNA and protein were strongly expressed in the biMs of the male eExG from E15.5 (Figure 1H) compared with that of the female (Figure 1I), concurrent with the onset of androgen-dependent urethral masculinization.[7] This dimorphic expression extends to E16.5 (Figures 1J and 1K; Figure S1B), at which the urethral tube begins to form prominently. To explore the possibility that *Mmp11* is

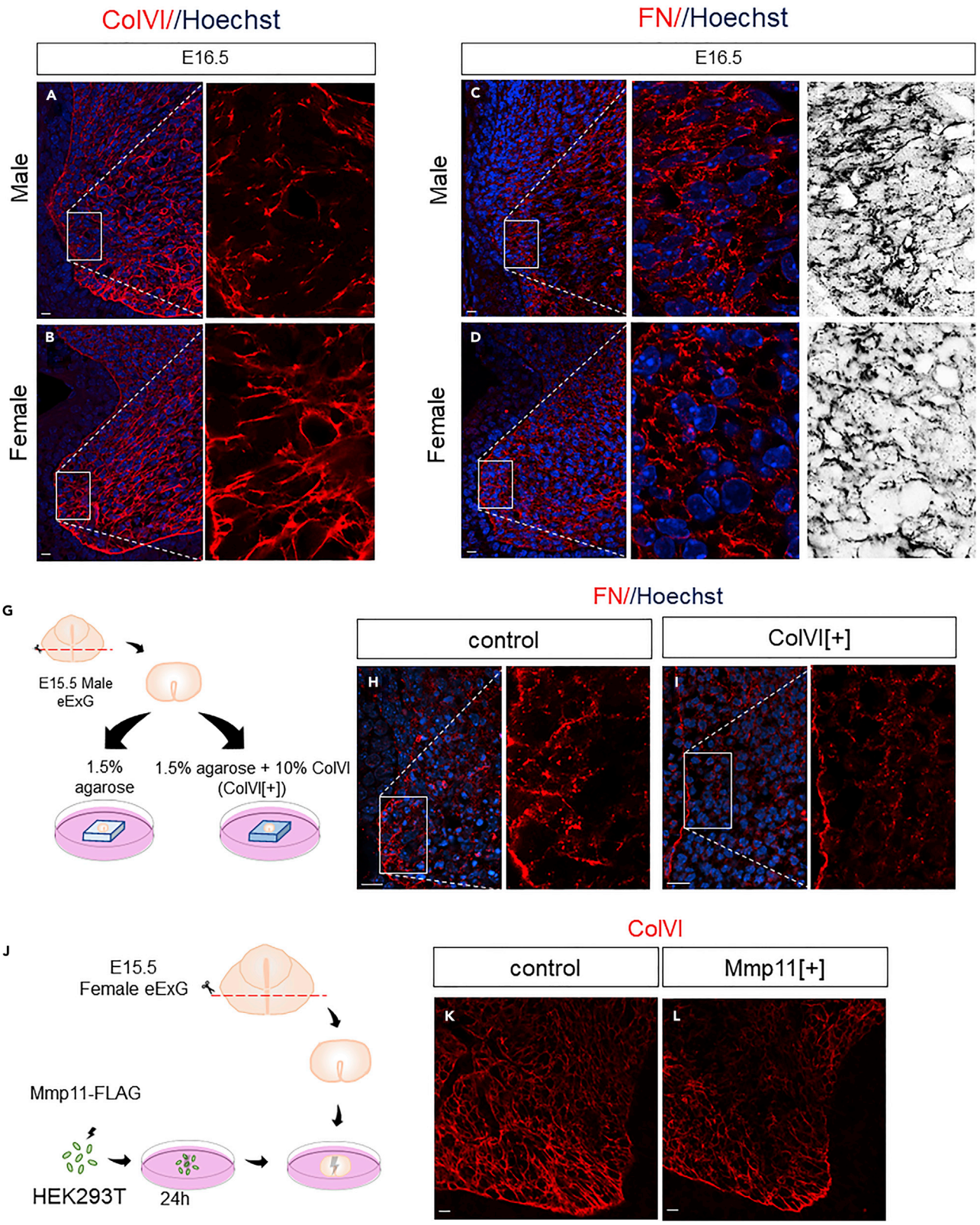
ColVI//Hoechst
E16.5
A
B
Male
Female
FN//Hoechst
E16.5
C
D
Male
Female
G
E15.5 Male
eExG
1.5%
agarose
1.5% agarose + 10% ColVI
(ColVI[+])
FN//Hoechst
control
ColVI[+]
H
I
J
E15.5
Female eExG
Mmp11-FLAG
HEK293T
24h
ColVI
control
Mmp11[+]
K
L

Figure 2. Requirement of MMP11 activity for ECM remodeling

[A–F] The ECM in the biMs is sexually dimorphic. See also Figure S2. (A and B) ColVI was downregulated in the biMs of E16.5 male mice (A) in contrast to the female (B). Scale bar: 10 μm. (C and D) Fibrillar deposition of FN was observed in the E16.5 male biMs (C). In contrast, FN was deposited in a ring-like pattern in the female (D). Scale bar: 10 μm. (E and F) Color-inverted photomicrographs of the FN network in E16.5 male (E) and female (F) biMs.

(G–L) Regulation of ColVI by *Mmp11* affects FN organization. Schematic diagram of eExG slices cultured on gels with exogenous ColVI. See also Figure S3G Schematic diagram of eExG slices cultured on gels with exogenous ColVI. (H and I) FN was deposited in a fibrillar pattern in the gel only set-up (H) and in a ring-like pattern in the presence of ColVI (I). Scale bar: 10 μm. (J) Schematic diagram of *Mmp11* overexpression set-up. (K and L) ColVI expression was reduced in eExG slices cultured in MMP11 conditioned medium (K) versus the control (L).Scale bar: 10 μm.

regulated by androgen, we treated wild-type female mice with testosterone proprionate (TP) during the masculinization window (E14.5-E15.5).[7] *Mmp11* was induced in the TP-treated female (Figures 1L and 1M), thus indicating that MMP11 is an androgen-inducible metalloproteinase that is highly expressed during urethral masculinization.

We next determined whether *Mmp11* is a downstream target of the androgen-dependent masculinization factor *MafB*. Conditional mesenchymal deletion of *MafB* resulted in the downregulation of the expression level of *Mmp11* in the biMs of the eExG (Figures 1N and 1O). To further confirm the necessity of *MafB* in *Mmp11* expression, we administered TP to *MafB* KO female mice and observed that its expression was not induced in the female mutant embryos even in the presence of androgen (Figure S1C). Moreover, the promoter region of *Mmp11* was highly conserved among mice, humans, and chimpanzees (Figure S1D), and we identified a histone 3 lysine 27 acetylation (H3K27ac) positive site in this region (GEO: GSE158279) (Figure 1P). The Maf recognition element (MARE) (Figure 1Q) was identified within this H3K27ac positive element by using the JASPAR database,[35] and ChIP-PCR analysis confirmed that MAFB was bound to this MARE site (Figure 1R). Taken together, these data suggest that, under androgen signaling, *MafB* regulates ECM remodeling through *Mmp11* during urethral masculinization.

Requirement of MMP11 activity for extracellular matrix remodeling

One of the known targets of MMP11 is the α3 chain of ColVI.[18] Thus, we analyzed its expression and observed that ColVI was downregulated in the biMs of both E15.5 and E16.5 male eExG (Figure 2A, Figure S2A). This reduction was not observed in the female (Figures 2B and S2A), suggesting that the changes in mesenchymal ColVI are required for the process of urethral masculinization. Loss of ColVI expression has been reported to be necessary for the proper deposition and organization of FN.[20–22] We next analyzed the expression of FN in the eExG and observed different FN deposition patterns between the male and the female biMs. Although a subtle difference between the sexes could be observed at E15.5 (Figure S2B), the sexually dimorphic FN deposition pattern became more prominent at E16.5. This difference was observed despite similar transcript expression levels between sexes (Figure S2C). FN fibrils were formed in the biMs at E16.5 (Figures 2C and 2E), coinciding with reduced ColVI expression; while a ring-like FN deposition was observed in the female biMs E16.5 (Figures 2D and 2F). These results suggest that mesenchymal ECM remodeling is required for androgen-driven urethral masculinization.

It has been reported that FN deposits in *Col6a1* null fibroblasts appear as streaked fibrils as opposed to the ring-like FN deposited in control cells.[20] To investigate whether the pattern of FN deposition is dependent on ColVI in the ECM, we analyzed the effect of exogenous ColVI on the pattern of FN deposition using an established eExG slice culture system.[5] eExG slices were cultured on gels supplemented with 10% ColVI (ColVI [+]) or without ColVI (control) for 24 h (Figure 2G). Similar to the female phenotype, slices cultured on ColVI [+] exhibited a ring-like deposition of FN (Figure 2H); whereas the streak-like pattern was observed in the control group (Figure 2I). The pattern of FN deposition in the biMs, therefore, is affected by the ColVI within the ECM environment.

To investigate whether MMP11 degrades ColVI in the biMs, we analyzed its expression in the biMs after culturing in MMP11-containing conditioned media. As MMP11 is secreted in its active form,[36] we transfected a *Mmp11* expression vector into HEK293 cells and confirmed the presence of the MMP11 protein by immunostaining and Western blotting (Figures S3A and S3B). Female eExG slices were cultured in either the MMP11 conditioned medium (Mmp11[+]) or control media for 24 h (Figure 2J). The deposition of ColVI was reduced in Mmp11[+] slices (Figure 2K) compared to the control (Figure 2L), suggesting that MMP11 in the biMs likely degrades ColVI during androgen-driven urethral masculinization. On the other hand, Collagen I, a major collagen in the eExG, was not affected by this treatment (Figure S2C), suggesting the substrate specificity of MMP11 to ColVI. The addition of MMP11, however, induced the fibrillar

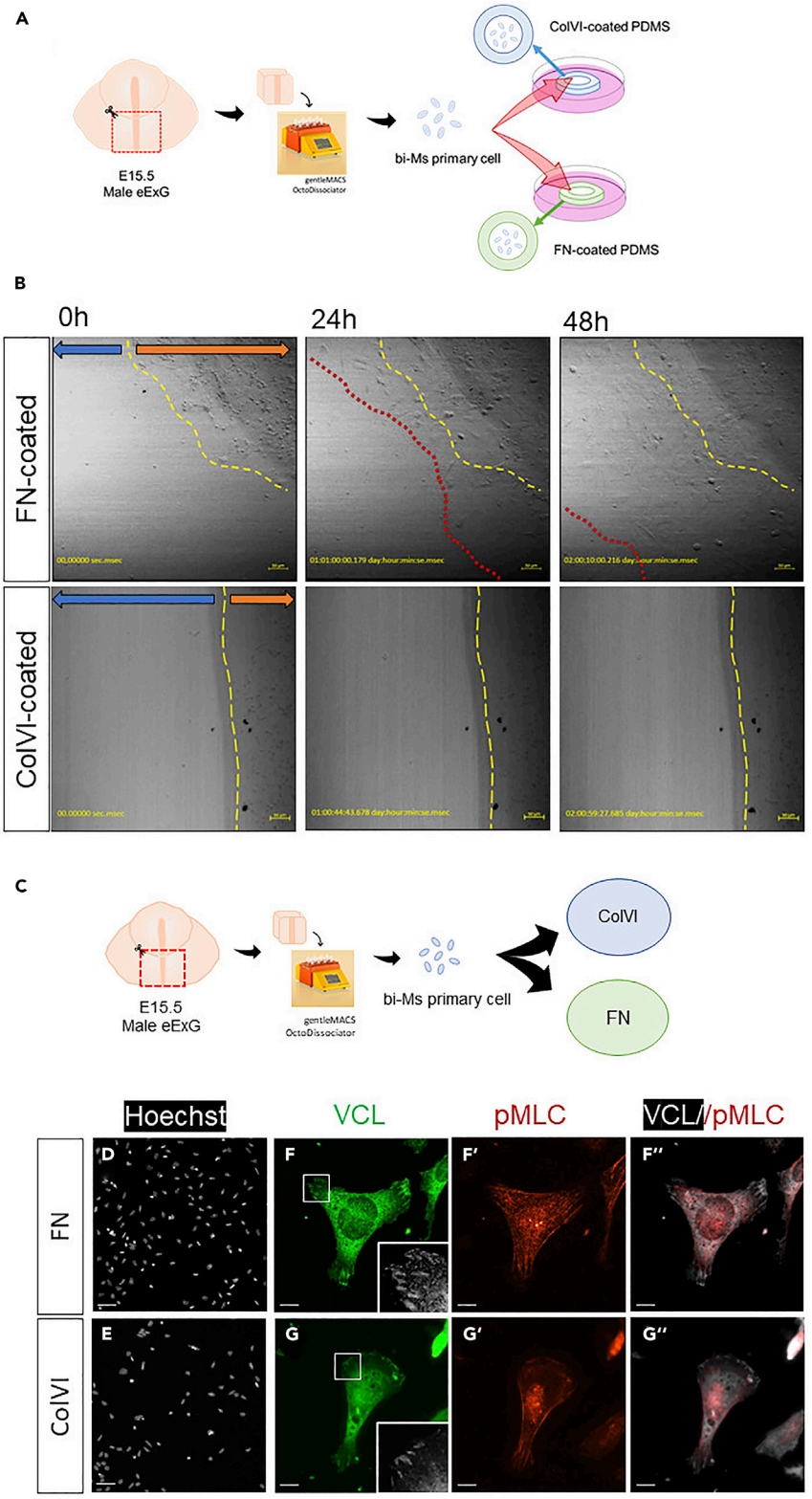

Figure 3. ECM remodeling is necessary for migration in the male biMs

(A and B) BiMs cells migrate more efficiently on FN rather than on ColVI. See also Videos S3 and S4. (A) Schematic diagram of primary cell migration assay. (B) Still images from live imaging video of biMs on either FN or ColVI. Images taken at 0,

Figure 3. *Continued*
24, and 48 h. Yellow dotted line marks the border between the coated and non-coated regions. Red dotted line indicates the end of migrating cells.
(C–G) BiMs cells cultured on FN possess prominent focal adhesions and stress fibers. (C) Schematic diagram of primary cell culture on either FN or ColVI. (D and E) More biMs cells adhered to FN (D) than to ColVI (E). Scale bar: 50 μm. (F and G) On FN, VCL (F) was strongly expressed on the edges of the cell, while pMLC (F′) was prominent throughout the cell body. On ColVI, VCL (G)-marked focal adhesions were smaller, and pMLC (G′) was restricted to the sides of the cell. F″ and G″ show merged image. Scale bar: 10 μm.

deposition of FN in the female biMs (Figure S2D). Altogether these data suggest that MMP11 remodels the ECM in the biMs by degrading ColVI which, in turn, alters the deposition pattern of FN during urethral masculinization.

MMP11-dependent extracellular matrix remodeling leads to cell migration in the male embryonic external genitalia

Since cell migration is necessary for urethral masculinization,[5] we next investigated whether ECM remodeling is critical for this process. In the absence of ColVI, both epithelial cells and neural crest cells have been reported to become more migratory on FN substrate.[21,22] To investigate whether MMP11-regulated ECM remodeling is required for cell migration in the eExG, we developed a migration assay using primary biMs cells. Following the recent methods of Hagiwara et al. (2021), polydimethylsiloxane (PDMS) rings were coated with either ColVI or FN, and cells were cultured within an inner well (Figure 3A).[37] After the cells have attached, we removed the PDMS sheets and observed the cells for 48 h. Live imaging analysis revealed that biMs cells migrated into the FN-coated region (Figure 3B; Video S3) within the first hour of culture. The cells proceeded to migrate efficiently into the coated region throughout the 48 h duration. In contrast, cells that were within the ColVI-coated region remained stationary (Figure 3B; Video S4).

To understand the mechanism leading to cell migration, we cultured biMs primary cells on either ColVI or FN (Figure 3C). After 24 h, a higher number of biMs cells was attached to the FN-coated well (Figures 3D and 3E). The presence of focal adhesions was marked using vinculin (VCL), and cell contractility was assessed by analyzing the expression of the phosphorylated myosin light chain (pMLC). Cells cultured on FN formed prominent lamellipodia that contained longer and more distinct focal adhesions (Figure 3F and 3F″), while those cultured on ColVI tended to form smaller adhesions (Figure 3G and 3G″) (Figure S4A). Contractile stress fibers were also more prominently expressed by cells cultured in the presence of FN (Figure 3F′ and 3F″) than on ColVI (Figure 3G′ and 3G″) (Figure S4A). These results suggest

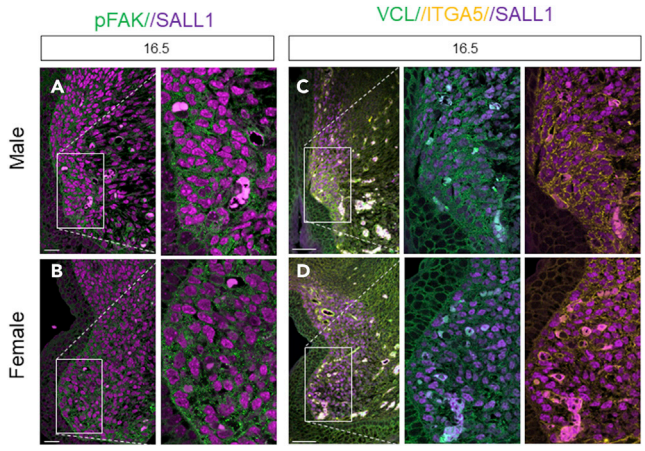

Figure 4. Focal adhesions are assembled in the male biMs
(A and B) pFAK was expressed more prominently in the male biMs (A) compared to the female (B). Scale bar: 50 μm.
(C and D) VCL and ITGA5 expressions co-localized in the male biMs (C), marked with SALL1, but not in the female (D). (C′ and D′) VCL expression in the biMs marked by SALL1. (C″ and D″) VCL expression in the biMs marked by SALL1. Scale bar: 50 μm. See also Figure S4.

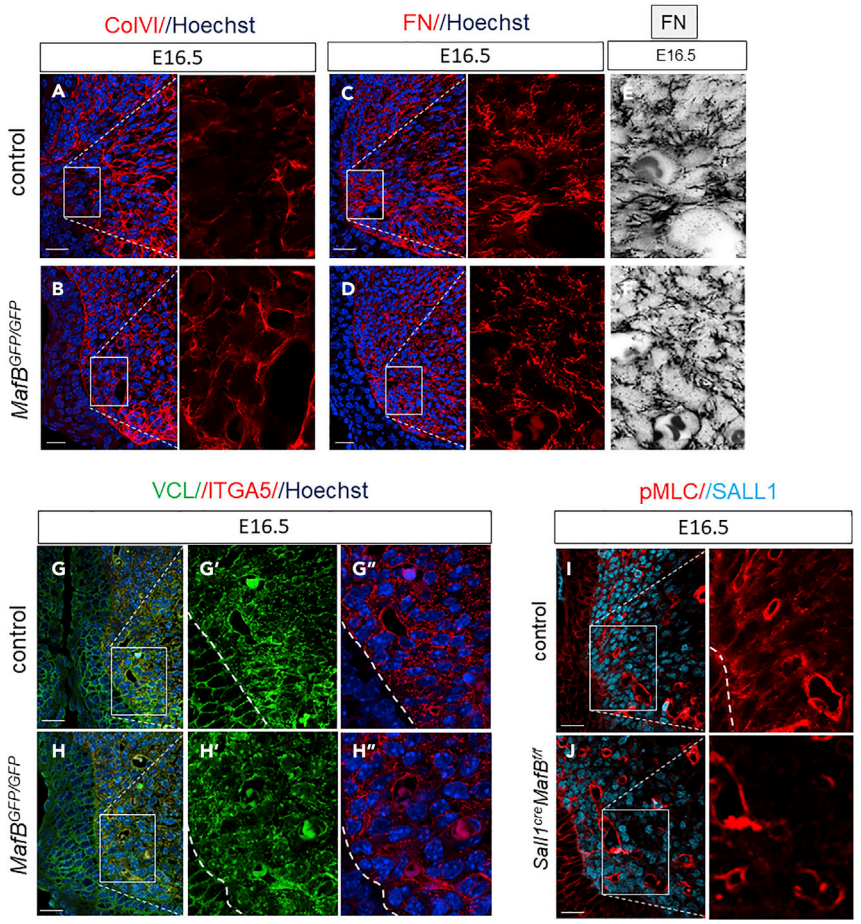

Figure 5. *MafB* is required for ECM-remodeling and subsequent cell migration

(A–D) The ECM environment of the *MafB* KO is similar to the female phenotype. (A and B) ColVI expression was reduced in the *MafB* KO (B) versus control (A). Scale bar: 50 μm. (C and D) FN expression in the *MafB* KO (D) was ring-like in pattern, in contrast to the fibrillar expression in the control male (C). Scale bar: 50 μm.

(E and F) Color-inverted photomicrographs of the FN network in control male (E) and MafB KO (F) biMs.

(G–J) Focal adhesion proteins and cell contractility are reduced in the *MafB* KO. (G and H) Focal adhesion proteins were downregulated in the *MafB* KO. (G′ and H′) VCL only. (G″ and H″) ITGA5/Hoechst. Scale bar: 50 μm. (I and J) pMLC was downregulated in the biMs of the *MafB* KO (J) compared to the control (I). Blood vessel expression (*) of pMLC remained the same. Scale bar: 50 μm. See also Figure S5.

that biMs cells require a shift from ColVI to FN to develop focal adhesions and contractility, leading to cell migration.

These *in vitro* data prompted us to investigate the cytoskeletal dynamics in the tissue during androgen-driven urethral masculinization. pMLC is upregulated in the male E16.5 eExG, compared to the female[5]; Figure S4B). The sexually dimorphic expression occurred from E15.5 (Figure S4B), concurrent with the onset of morphologically dimorphic eExG development. Furthermore, focal adhesion markers - phosphorylated-focal adhesion kinase (pFAK), VCL, and integrin α5 (ITGA5) - were also expressed prominently in the male biMs but not in females (Figures 4A–4D). The sexually dimorphic expression was observed from E15.5 (Figures S4C and S4D). Collectively, these findings suggest that to form the urethral tube during masculinization, MMP11-dependent ECM remodeling in the biMs is required for the MafB-positive cells to acquire a migratory state.

MafB drives cell migration via MMP11-dependent extracellular matrix remodeling

As mentioned, *MafB* regulates *Mmp11* expression in the biMs. To reinforce the significance of upstream *MafB* signaling, we analyzed the expressions of several ECM proteins, cell-matrix adhesion markers, and

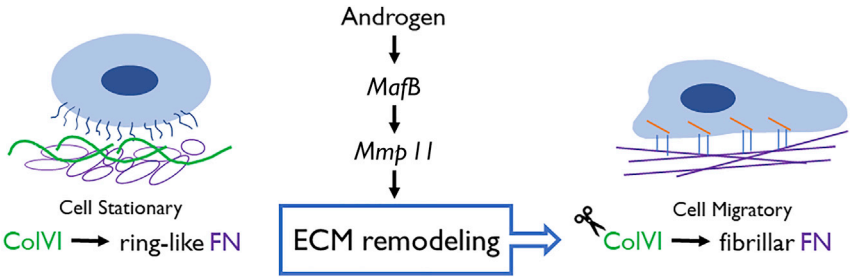

Figure 6. Androgen-regulated *MafB* drives cell migration via *Mmp11*-dependent ECM remodeling
Cleavage of ColVI (green) by *MafB*-induced MMP11 results in the fibrillar organization of FN (purple). This change in the ECM substrate allows the cells of the biMs to adapt migratory characteristics, leading to the masculinization of the urethral tube.

actomyosin activity in the *MafB* KO mice. A *MafB*-GFP knock-in mouse line ($MafB^{GFP/+}$) was utilized to identify the *MafB*-expressing biMs cells (Figure S5). Expression of ColVI remained in the biMs of the KO mouse (Figures 5A and 5B) and FN was observed in a ring-like pattern (Figures 5C–5F), which was similar to the female ECM microenvironment. Moreover, pMLC, VCL, and ITGA5 were downregulated in the absence of MafB (Figures 5G–5J). These results indicate that *MafB* regulates cell migration through MMP11-dependent ECM remodeling in the biMs.

DISCUSSION

Androgens govern the development of the male reproductive organs. Epithelial androgen signaling regulates cell proliferation, differentiation, and survival during the development of the prostate, epididymis, and seminal vesicles.[38] While mesenchymal androgen receptor (AR) signaling is necessary for epithelial cell proliferation and differentiation in the prostate gland,[39] the role of mesenchymal androgen signaling during male external genitalia development has yet to be elucidated. Here, we demonstrate that local ECM remodeling, under mesenchymal androgen signaling, is essential during eExG development. Androgen-MafB drives cell migration through the regulation of MMP11-dependent ECM remodeling: MMP11-degradation of ColVI in the mesenchyme leads to the fibrillar deposition of FN, and this allows the biMs cells to form focal adhesions required for sexually dimorphic cell migration (Figure 6).

MafB is a regulator of *Mmp11* under androgen signaling

Androgens regulate MMP expression in prostate and bladder cancers; however, its regulatory effect is context-, type-, and dose-dependent.[40–42] While it is generally accepted that AR signaling can stimulate MMP activity,[40,43,44] it has also been reported to downregulate the expression of MMPs through Ets transcription factors.[45] AR induces the activity of target genes through transcription factors such as SRY, SP1, and the Activator Protein-1 (AP-1) super family.[1,46–48] The AP-1 superfamily consists of the Jun, Fos, and Maf families.[1,49,50] A highly conserved region, which includes a binding site for Jun/Fos dimers, is present in the *cis*-regulatory elements of the promoter regions of several MMPs.[51,52] MMP11 possesses an additional AP-1 site in its promoter region that, while still responsive to Jun and Fos, is not an exact match.[53] In addition, MMP3, which belongs to the same MMP group as MMP11, similarly possesses this slightly divergent AP-1 site.[53] In chondrocytes, MafB has been reported to stimulate MMP3/13 expression in response to retinoic acid signaling,[53,54] suggesting a possibility of MafB as a regulator not only of MMP11, but of stromelysins. Here, we report that a MARE is present in the promoter region of *Mmp11* and that *MafB*, another member of the AP-1 family of transcription factors, binds to this site during urethral masculinization. Since there are currently no known *Mmp11* regulators during development, androgen-regulated *MafB* is the first suitable candidate as an upstream regulator of *Mmp11*.

Androgen-driven cell migration via extracellular matrix remodeling during organogenesis

In the prostate, androgens initiate ductal growth and cell differentiation.[55,56] In the Wolffian duct, androgens are required for cell differentiation and proliferation.[57] While androgen is known as the master regulator for sexually dimorphic reproductive organ formation, the mechanism through which it orchestrates organogenesis has yet to be defined. We previously reported that male-specific mesenchymal cell

dynamics is indispensable during androgen-dependent urethral masculinization.[1,4,58] Here, we report that cell migration is defective in the *MafB* mutant mesenchyme, indicating that androgen-regulated *MafB* is required for mesenchymal cell migration during eExG development.

Organogenesis is generally associated with high levels of tissue remodeling and cell migration.[59] During gut looping, the migration of the epithelial lateral plate mesodermal cells requires the loss of laminin through MMP activity,[60] and the direction of looping is determined through asymmetric ECM deposition in the mesenchyme.[61] Extensive remodeling of the ECM also occurs during the development of the lung, the tooth, and the palate.[62,63] Our data demonstrate remodeling of the ECM alongside urethral tube development: MMP11 degrades ColVI, resulting in the fibrillar deposition of FN. It has been suggested that this is due to the competitive binding of ColVI for integrin β1 which prevents fibrillogenesis.[20,21] We observed increased focal adhesion assembly and cell contractility in the male biMs and also in cells cultured with FN. FN has been reported to promote the formation of focal adhesions and cell migration.[22,64] In the lung, FN polymerization is required for small airway epithelial cell migration.[65] Myoblast cells have also been shown to migrate with persistent directionality on FN but not on gelatin.[66] In addition, polymerization of soluble FN into fibrils has been reported to be required to generate cytoskeletal tension.[67] It has further been suggested that a low ColVI/high FN environment leads to an increase in the phosphorylation of MLC through alterations in the calcium pathway.[21] Lastly, in the eExG, F-actin stress fibers and actomyosin contractility increase in response to androgens.[4,5] Hormone-dependent ECM remodeling has also been previously reported during tadpole metamorphosis: MMP11 cleaves the basement membrane in response to thyroid hormone during intestinal development.[16,68] We have shown that MMP11 is an androgen-dependent metalloproteinase in the eExG. Intriguingly, androgen exposure is sufficient to induce cell migration in female eExG slice cultures.[5] These all support our finding that MMP11-regulated ECM remodeling is vital in androgen-driven mesenchymal cell migration during eExG sexual differentiation.

Tissue fusion is classically studied through neural tube formation, palate morphogenesis, and heart development. Among these three, mesenchymal cell migration is most well-studied during heart development, focusing on neural crest cells as a model.[69] Our study introduces the development of the external genitalia as an alternative model for investigating mesenchymal cellular processes that occur during tissue fusion. We report that this process is under androgen regulation. Several other organs suggest links between androgen signaling, *MafB* expression, and tissue remodeling. Organs of the cardiovascular system undergo androgen-dependent development,[70] and *MafB* is a critical transcription factor for the development of the highly migratory cardiac neural crest cell.[71] Similarly, the development of the CNS has also been reported to be sexually dimorphic.[72,73] In this system, *MafB* is required for hindbrain segmentation and regional specification.[74] It will be interesting to investigate whether androgen-MafB signaling can induce cell migration via MMP11-dependent ECM remodeling in other systems.

Limitations of the study

In this study, we elucidated the role of androgen-regulated *MafB* during cell migration using the masculinization of the mouse urethra as a model, and our *in vitro* assays on migration utilized mouse primary cells. Whether the same mechanism occurs in other mammals, including humans, remains to be explored. Furthermore, *MafB* is also expressed in other organs. Investigating downstream events to *MafB* in these systems would contribute to the generality of our proposed mechanism.

STAR★METHODS

Detailed methods are provided in the online version of this paper and include the following:

- KEY RESOURCES TABLE
- RESOURCE AVAILABILITY
  - Lead contact
  - Materials availability statement
  - Data availability statement
- EXPERIMENTAL MODEL AND SUBJECT DETAILS
- METHOD DETAILS
  - Histological analyses and imaging
  - Chromatin immunoprecipitation (ChIP) assay and ChIP-Seq analysis

- Primary cell migration assay and culture
- Mmp11 overexpression, eExG slice culture, and exogenous collagen 6 assays
- RNA sequencing and qPCR analysis

- QUANTIFICATION AND STATISTICAL ANALYSIS

SUPPLEMENTAL INFORMATION

Supplemental information can be found online at https://doi.org/10.1016/j.isci.2022.105609.

ACKNOWLEDGMENTS

We would like to thank Dr. Suneel Apte and Dr. Timothy Mead of the Lerner's Research Institute; the Laboratory Animal Center, the Department of Immunology, and the Central Research Facility of the Wakayama Medical University; and Mr. Ryouya Taniguchi of Kindai University for their advice and technical support. We would also like to acknowledge Tomiko Iba, Yugi Rim, and the members of the Department of Developmental Genetics for their invaluable support. This work was supported by the Japan Society for the Promotion of Science KAKENHI (17H06432, 18K06837, 18K06938, 21K06822, and 21K19538) and the Monbukagakusho Scholarship from the Japanese Ministry of Education, Culture, Sports, Science, and Technology.

AUTHOR CONTRIBUTIONS

Conceptualization: K.S. and G.Y.; methodology: M.C.A., K.S., and A.R.A.; investigation: M.C.A., D.K., and Y.H.; writing – original draft, visualization: M.C.A.; writing – review and editing: K.S. and G.Y.; resources: S.H., T.K., K.Y., and S.T.; supervision: K.S. and G.Y.; funding acquisition: K.S. and G.Y.

DECLARATION OF INTERESTS

The authors have nothing to declare.

INCLUSION AND DIVERSITY

We support inclusive, diverse, and equitable conduct of research.

Received: May 26, 2022
Revised: October 4, 2022
Accepted: November 14, 2022
Published: December 22, 2022

REFERENCES

1. Matsushita, S., Suzuki, K., Murashima, A., Kajioka, D., Acebedo, A.R., Miyagawa, S., Haraguchi, R., Ogino, Y., and Yamada, G. (2018). Regulation of masculinization: androgen signalling for external genitalia development. Nat. Rev. Urol. *15*, 358–368. https://doi.org/10.1038/s41585-018-0008-y.

2. Matsushita, S., Suzuki, K., Ogino, Y., Hino, S., Sato, T., Suyama, M., Matsumoto, T., Omori, A., Inoue, S., and Yamada, G. (2016). Androgen regulates mafb expression through its 3'UTR during mouse urethral masculinization. Endocrinology *157*, 844–857. https://doi.org/10.1210/en.2015-1586.

3. Suzuki, K., Numata, T., Suzuki, H., Raga, D.D., Ipulan, L.A., Yokoyama, C., Matsushita, S., Hamada, M., Nakagata, N., Nishinakamura, R., et al. (2014). Sexually dimorphic expression of Mafb regulates masculinization of the embryonic urethral formation. Proc. Natl. Acad. Sci. USA *111*, 16407–16412. https://doi.org/10.1073/pnas.1413273111.

4. Liu, L., Suzuki, K., Chun, E., Murashima, A., Sato, Y., Nakagata, N., Fujimori, T., Yonemura, S., He, W., and Yamada, G. (2017). Androgen regulates dimorphic F-actin assemblies in the genital organogenesis. Sex Dev. *11*, 190–202. https://doi.org/10.1159/000477452.

5. Acebedo, A.R., Suzuki, K., Hino, S., Alcantara, M.C., Sato, Y., Haga, H., Matsumoto, K.I., Nakao, M., Shimamura, K., Takeo, T., et al. (2019). Mesenchymal actomyosin contractility is required for androgen-driven urethral masculinization in mice. Commun. Biol. *2*, 95. https://doi.org/10.1038/s42003-019-0336-3.

6. Suzuki, H., Matsushita, S., Suzuki, K., and Yamada, G. (2017). 5α-Dihydrotestosterone negatively regulates cell proliferation of the periurethral ventral mesenchyme during urethral tube formation in the murine male genital tubercle. Andrology *5*, 146–152. https://doi.org/10.1111/andr.12241.

7. Zheng, Z., Armfield, B.A., and Cohn, M.J. (2015). Timing of androgen receptor disruption and estrogen exposure underlies a spectrum of congenital penile anomalies. Proc. Natl. Acad. Sci. USA *112*, E7194–E7203. https://doi.org/10.1073/pnas.1515981112.

8. Larkins, C.E., Enriquez, A.B., and Cohn, M.J. (2016). Spatiotemporal dynamics of androgen signaling underlie sexual differentiation and congenital malformations of the urethra and vagina. Proc. Natl. Acad. Sci. USA *113*, E7510–E7517. https://doi.org/10.1073/pnas.1610471113.

9. Yamada, K.M., and Sixt, M. (2019). Mechanisms of 3D cell migration. Nat. Rev. Mol. Cell Biol. *20*, 738–752. https://doi.org/10.1038/s41580-019-0172-9.

10. Hartman, C.D., Isenberg, B.C., Chua, S.G., and Wong, J.Y. (2017). Extracellular matrix type modulates cell migration on mechanical gradients. Exp. Cell Res. *359*, 361–366. https://doi.org/10.1016/j.yexcr.2017.08.018.

11. Page-McCaw, A., Ewald, A.J., and Werb, Z. (2007). Matrix metalloproteinases and the regulation of tissue remodelling. Nat. Rev.

Mol. Cell Biol. *8*, 221–233. https://doi.org/10.1038/nrm2125.

12. Basset, P., Bellocq, J.P., Wolf, C., Stoll, I., Hutin, P., Limacher, J.M., Podhajcer, O.L., Chenard, M.P., Rio, M.C., and Chambon, P. (1990). A novel metalloproteinase gene specifically expressed in stromal cells of breast carcinomas. Nature *348*, 699–704. https://doi.org/10.1038/348699a0.

13. Rio, M.C. (2005). From a unique cell to metastasis is a long way to go: clues to stromelysin-3 participation. Biochimie *87*, 299–306. https://doi.org/10.1016/j.biochi.2004.11.016.

14. Lefebvre, O., Wolf, C., Limacher, J.M., Hutin, P., Wendling, C., LeMeur, M., Basset, P., and Rio, M.C. (1992). The breast cancer-associated stromelysin-3 gene is expressed during mouse mammary gland apoptosis. J. Cell Biol. *119*, 997–1002. https://doi.org/10.1083/jcb.119.4.997.

15. Lefebvre, O., Régnier, C., Chenard, M.P., Wendling, C., Chambon, P., Basset, P., and Rio, M.C. (1995). Developmental expression of mouse stromelysin-3 mRNA. Development *121*, 947–955.

16. Ishizuya-Oka, A., Li, Q., Amano, T., Damjanovski, S., Ueda, S., and Shi, Y.B. (2000). Requirement for matrix metalloproteinase stromelysin-3 in cell migration and apoptosis during tissue remodeling in Xenopus laevis. J. Cell Biol. *150*, 1177–1188. https://doi.org/10.1083/jcb.150.5.1177.

17. Peruzzi, D., Mori, F., Conforti, A., Lazzaro, D., De Rinaldis, E., Ciliberto, G., La Monica, N., and Aurisicchio, L. (2009). MMP11: a novel target antigen for cancer immunotherapy. Clin. Cancer Res. *15*, 4104–4113. https://doi.org/10.1158/1078-0432.CCR-08-3226.

18. Motrescu, E.R., Blaise, S., Etique, N., Messaddeq, N., Chenard, M.P., Stoll, I., Tomasetto, C., and Rio, M.C. (2008). Matrix metalloproteinase-11/stromelysin-3 exhibits collagenolytic function against collagen VI under normal and malignant conditions. Oncogene *27*, 6347–6355. https://doi.org/10.1038/onc.2008.218.

19. Keene, D.R., Engvall, E., and Glanville, R.W. (1988). Ultrastructure of type VI collagen in human skin and cartilage suggests an anchoring function for this filamentous network. J. Cell Biol. *107*, 1995–2006. https://doi.org/10.1083/jcb.107.5.1995.

20. Sabatelli, P., Bonaldo, P., Lattanzi, G., Braghetta, P., Bergamin, N., Capanni, C., Mattioli, E., Columbaro, M., Ognibene, A., Pepe, G., et al. (2001). Collagen VI deficiency affects the organization of fibronectin in the extracellular matrix of cultured fibroblasts. Matrix Biol. *20*, 475–486. https://doi.org/10.1016/s0945-053x(01)00160-3.

21. Groulx, J.F., Gagné, D., Benoit, Y.D., Martel, D., Basora, N., and Beaulieu, J.F. (2011). Collagen VI is a basement membrane component that regulates epithelial cell-fibronectin interactions. Matrix Biol. *30*, 195–206. https://doi.org/10.1016/j.matbio.2011.03.002.

22. Nishida, S., Yoshizaki, H., Yasui, Y., Kuwahara, T., Kiyokawa, E., and Kohno, M. (2018). Collagen VI suppresses fibronectin-induced enteric neural crest cell migration by downregulation of focal adhesion proteins. Biochem. Biophys. Res. Commun. *495*, 1461–1467. https://doi.org/10.1016/j.bbrc.2017.11.184.

23. Rozario, T., and DeSimone, D.W. (2010). The extracellular matrix in development and morphogenesis: a dynamic view. Dev. Biol. *341*, 126–140. https://doi.org/10.1016/j.ydbio.2009.10.026.

24. Boucaut, J.C., Darribère, T., Boulekbache, H., and Thiery, J.P. (1984). Prevention of gastrulation but not neurulation by antibodies to fibronectin in amphibian embryos. Nature *307*, 364–367. https://doi.org/10.1038/307364a0.

25. Latimer, A., and Jessen, J.R. (2010). Extracellular matrix assembly and organization during zebrafish gastrulation. Matrix Biol. *29*, 89–96. https://doi.org/10.1016/j.matbio.2009.10.002.

26. Trinh, L.A., and Stainier, D.Y.R. (2004). Fibronectin regulates epithelial organization during myocardial migration in zebrafish. Dev. Cell *6*, 371–382. https://doi.org/10.1016/s1534-5807(04)00063-2.

27. Boucaut, J.C., Johnson, K.E., Darribère, T., Shi, D.L., Riou, J.F., Bache, H.B., and Delarue, M. (1990). Fibronectin-rich fibrillar extracellular matrix controls cell migration during amphibian gastrulation. Int. J. Dev. Biol. *34*, 139–147.

28. Rozario, T., Dzamba, B., Weber, G.F., Davidson, L.A., and DeSimone, D.W. (2009). The physical state of fibronectin matrix differentially regulates morphogenetic movements in vivo. Dev. Biol. *327*, 386–398. https://doi.org/10.1016/j.ydbio.2008.12.025.

29. Davidson, L.A., Dzamba, B.D., Keller, R., and Desimone, D.W. (2008). Live imaging of cell protrusive activity, and extracellular matrix assembly and remodeling during morphogenesis in the frog, Xenopus laevis. Dev. Dyn. *237*, 2684–2692. https://doi.org/10.1002/dvdy.21600.

30. Davidson, L.A., Keller, R., and DeSimone, D.W. (2004). Assembly and remodeling of the fibrillar fibronectin extracellular matrix during gastrulation and neurulation in Xenopus laevis. Dev. Dyn. *231*, 888–895. https://doi.org/10.1002/dvdy.20217.

31. Tang, Q., Li, L., Jin, C., Lee, J.M., and Jung, H.S. (2015). Role of region-distinctive expression of Rac1 in regulating fibronectin arrangement during palatal shelf elevation. Cell Tissue Res. *361*, 857–868. https://doi.org/10.1007/s00441-015-2169-9.

32. Schwarzbauer, J.E., and DeSimone, D.W. (2011). Fibronectins, their fibrillogenesis, and in vivo functions. Cold Spring Harb. Perspect. Biol. *3*, a005041. https://doi.org/10.1101/cshperspect.a005041.

33. Loganathan, R., Potetz, B.R., Rongish, B.J., and Little, C.D. (2012). Spatial anisotropies and temporal fluctuations in extracellular matrix network texture during early embryogenesis. PLoS One *7*, e38266. https://doi.org/10.1371/journal.pone.0038266.

34. Miyagawa, S., Satoh, Y., Haraguchi, R., Suzuki, K., Iguchi, T., Taketo, M.M., Nakagata, N., Matsumoto, T., Takeyama, K.i., Kato, S., and Yamada, G. (2009). Genetic interactions of the androgen and Wnt/beta-catenin pathways for the masculinization of external genitalia. Mol. Endocrinol. *23*, 871–880. https://doi.org/10.1210/me.2008-0478.

35. Fornes, O., Castro-Mondragon, J.A., Khan, A., van der Lee, R., Zhang, X., Richmond, P.A., Modi, B.P., Correard, S., Gheorghe, M., Baranašić, D., et al. (2020). Jaspar 2020: update of the open-access database of transcription factor binding profiles. Nucleic Acids Res. *48*, D87–D92. https://doi.org/10.1093/nar/gkz1001.

36. Pei, D., and Weiss, S.J. (1995). Furin-dependent intracellular activation of the human stromelysin-3 zymogen. Nature *375*, 244–247. https://doi.org/10.1038/375244a0.

37. Hagiwara, M., Maruyama, H., Akiyama, M., Koh, I., and Arai, F. (2021). Weakening of resistance force by cell-ECM interactions regulate cell migration directionality and pattern formation. Commun. Biol. *4*, 808. https://doi.org/10.1038/s42003-021-02350-4.

38. Murashima, A., Kishigami, S., Thomson, A., and Yamada, G. (2015). Androgens and mammalian male reproductive tract development. Biochim. Biophys. Acta *1849*, 163–170. https://doi.org/10.1016/j.bbagrm.2014.05.020.

39. Cunha, G.R., and Chung, L.W. (1981). Stromal-epithelial interactions–I. Induction of prostatic phenotype in urothelium of testicular feminized (Tfm/y) mice. J. Steroid Biochem. *14*, 1317–1324. https://doi.org/10.1016/0022-4731(81)90338-1.

40. Liao, X., Thrasher, J.B., Pelling, J., Holzbeierlein, J., Sang, Q.X.A., and Li, B. (2003). Androgen stimulates matrix metalloproteinase-2 expression in human prostate cancer. Endocrinology *144*, 1656–1663. https://doi.org/10.1210/en.2002-0157.

41. Lin, C., Lin, W., Yeh, S., Li, L., and Chang, C. (2015). Infiltrating neutrophils increase bladder cancer cell invasion via modulation of androgen receptor (AR)/MMP13 signals. Oncotarget *6*, 43081–43089. https://doi.org/10.18632/oncotarget.5638.

42. Mountain, D.J.H., Freeman, B.M., Kirkpatrick, S.S., Beddies, J.W., Arnold, J.D., Freeman, M.B., Goldman, M.H., Stevens, S.L., Klein, F.A., and Grandas, O.H. (2013). Androgens regulate MMPs and the cellular processes of intimal hyperplasia. J. Surg. Res. *184*, 619–627. https://doi.org/10.1016/j.jss.2013.05.070.

43. Hara, T., Miyazaki, H., Lee, A., Tran, C.P., and Reiter, R.E. (2008). Androgen receptor and invasion in prostate cancer. Cancer Res. *68*, 1128–1135. https://doi.org/10.1158/0008-5472.CAN-07-1929.

44. Pang, S.T., Flores-Morales, A., Skoog, L., Chuan, Y.C., Nordstedt, G., and Pousette, A.

(2004). Regulation of matrix metalloproteinase 13 expression by androgen in prostate cancer. Oncol. Rep. *11*, 1187–1192.

45. Schneikert, J., Peterziel, H., Defossez, P.A., Klocker, H., de Launoit, Y., and Cato, A.C. (1996). Androgen receptor-Ets protein interaction is a novel mechanism for steroid hormone-mediated down-modulation of matrix metalloproteinase expression. J. Biol. Chem. *271*, 23907–23913. https://doi.org/10.1074/jbc.271.39.23907.

46. Kajioka, D., Suzuki, K., Matsushita, S., Hino, S., Sato, T., Takada, S., Isono, K., Takeo, T., Kajimoto, M., Nakagata, N., et al. (2021). Sexual fate of murine external genitalia development: conserved transcriptional competency for male-biased genes in both sexes. Proc. Natl. Acad. Sci. USA *118*. e2024067118. https://doi.org/10.1073/pnas.2024067118.

47. Yuan, X., Lu, M.L., Li, T., and Balk, S.P. (2001). SRY interacts with and negatively regulates androgen receptor transcriptional activity. J. Biol. Chem. *276*, 46647–46654. https://doi.org/10.1074/jbc.M108404200.

48. Takai, H., Nakayama, Y., Kim, D.S., Arai, M., Araki, S., Mezawa, M., Nakajima, Y., Kato, N., Masunaga, H., and Ogata, Y. (2007). Androgen receptor stimulates bone sialoprotein (BSP) gene transcription via cAMP response element and activator protein 1/glucocorticoid response elements. J. Cell. Biochem. *102*, 240–251. https://doi.org/10.1002/jcb.21297.

49. Koochekpour, S. (2010). Androgen receptor signaling and mutations in prostate cancer. Asian J. Androl. *12*, 639–657. https://doi.org/10.1038/aja.2010.89.

50. Eychène, A., Rocques, N., and Pouponnot, C. (2008). A new MAFia in cancer. Nat. Rev. Cancer *8*, 683–693. https://doi.org/10.1038/nrc2460.

51. White, L.A., and Brinckerhoff, C.E. (1995). Two activator protein-1 elements in the matrix metalloproteinase-1 promoter have different effects on transcription and bind Jun D, c-Fos, and Fra-2. Matrix Biol. *14*, 715–725. https://doi.org/10.1016/s0945-053x(05)80014-9.

52. Chamberlain, S.H., Hemmer, R.M., and Brinckerhoff, C.E. (1993). Novel phorbol ester response region in the collagenase promoter binds Fos and Jun. J. Cell. Biochem. *52*, 337–351. https://doi.org/10.1002/jcb.240520310.

53. Benbow, U., and Brinckerhoff, C.E. (1997). The AP-1 site and MMP gene regulation: what is all the fuss about? Matrix Biol. *15*, 519–526. https://doi.org/10.1016/s0945-053x(97)90026-3.

54. Zhang, Y., and Ross, A.C. (2013). Retinoic acid and the transcription factor MafB act together and differentially to regulate aggrecan and matrix metalloproteinase gene expression in neonatal chondrocytes. J. Cell. Biochem. *114*, 471–479. https://doi.org/10.1002/jcb.24387.

55. Francis, J.C., and Swain, A. (2018). Prostate organogenesis. Cold Spring Harb. Perspect. Med. *8*, a030353. https://doi.org/10.1101/cshperspect.a030353.

56. Lasnitzki, I., and Mizuno, T. (1977). Induction of the rat prostate gland by androgens in organ culture. J. Endocrinol. *74*, 47–55. https://doi.org/10.1677/joe.0.0740047.

57. Shaw, G., and Renfree, M.B. (2014). Wolffian duct development. Sex Dev. *8*, 273–280. https://doi.org/10.1159/000363432.

58. Yamada, G., Suzuki, K., Haraguchi, R., Miyagawa, S., Satoh, Y., Kamimura, M., Nakagata, N., Kataoka, H., Kuroiwa, A., and Chen, Y. (2006). Molecular genetic cascades for external genitalia formation: an emerging organogenesis program. Dev. Dyn. *235*, 1738–1752. https://doi.org/10.1002/dvdy.20807.

59. Aman, A., and Piotrowski, T. (2010). Cell migration during morphogenesis. Dev. Biol. *341*, 20–33. https://doi.org/10.1016/j.ydbio.2009.11.014.

60. Yin, C., Kikuchi, K., Hochgreb, T., Poss, K.D., and Stainier, D.Y.R. (2010). Hand2 regulates extracellular matrix remodeling essential for gut-looping morphogenesis in zebrafish. Dev. Cell *18*, 973–984. https://doi.org/10.1016/j.devcel.2010.05.009.

61. Kurpios, N.A., Ibañes, M., Davis, N.M., Lui, W., Katz, T., Martin, J.F., Izpisúa Belmonte, J.C., and Tabin, C.J. (2008). The direction of gut looping is established by changes in the extracellular matrix and in cell:cell adhesion. Proc. Natl. Acad. Sci. USA *105*, 8499–8506. https://doi.org/10.1073/pnas.0803578105.

62. Zhou, Y., Horowitz, J.C., Naba, A., Ambalavanan, N., Atabai, K., Balestrini, J., Bitterman, P.B., Corley, R.A., Ding, B.S., Engler, A.J., et al. (2018). Extracellular matrix in lung development, homeostasis and disease. Matrix Biol. *73*, 77–104. https://doi.org/10.1016/j.matbio.2018.03.005.

63. Wang, X., Li, C., Zhu, Z., Yuan, L., Chan, W.Y., and Sha, O. (2020). Extracellular matrix remodeling during palate development. Organogenesis *16*, 43–60. https://doi.org/10.1080/15476278.2020.1735239.

64. Vedula, S.R.K., Leong, M.C., Lai, T.L., Hersen, P., Kabla, A.J., Lim, C.T., and Ladoux, B. (2012). Emerging modes of collective cell migration induced by geometrical constraints. Proc. Natl. Acad. Sci. USA *109*, 12974–12979. https://doi.org/10.1073/pnas.1119313109.

65. Hocking, D.C., and Chang, C.H. (2003). Fibronectin matrix polymerization regulates small airway epithelial cell migration. Am. J. Physiol. Lung Cell Mol. Physiol. *285*, L169–L179. https://doi.org/10.1152/ajplung.00371.2002.

66. Vaz, R., Martins, G.G., Thorsteinsdóttir, S., and Rodrigues, G. (2012). Fibronectin promotes migration, alignment and fusion in an in vitro myoblast cell model. Cell Tissue Res. *348*, 569–578. https://doi.org/10.1007/s00441-012-1364-1.

67. Hocking, D.C., Sottile, J., and Langenbach, K.J. (2000). Stimulation of integrin-mediated cell contractility by fibronectin polymerization. J. Biol. Chem. *275*, 10673–10682. https://doi.org/10.1074/jbc.275.14.10673.

68. Damjanovski, S., Amano, T., Li, Q., Ueda, S., Shi, Y.B., and Ishizuya-Oka, A. (2000). Role of ECM remodeling in thyroid hormone-dependent apoptosis during anuran metamorphosis. Ann. N. Y. Acad. Sci. *926*, 180–191. https://doi.org/10.1111/j.1749-6632.2000.tb05611.x.

69. Theveneau, E., and Mayor, R. (2011). Can mesenchymal cells undergo collective cell migration? The case of the neural crest. Cell Adh. Migr. *5*, 490–498. https://doi.org/10.4161/cam.5.6.18623.

70. Shi, W., Sheng, X., Dorr, K.M., Hutton, J.E., Emerson, J.I., Davies, H.A., Andrade, T.D., Wasson, L.K., Greco, T.M., Hashimoto, Y., et al. (2021). Cardiac proteomics reveals sex chromosome-dependent differences between males and females that arise prior to gonad formation. Dev. Cell *56*, 3019–3034.e7. https://doi.org/10.1016/j.devcel.2021.09.022.

71. Tani-Matsuhana, S., Vieceli, F.M., Gandhi, S., Inoue, K., and Bronner, M.E. (2018). Transcriptome profiling of the cardiac neural crest reveals a critical role for MafB. Dev. Biol. *444*, S209–S218. https://doi.org/10.1016/j.ydbio.2018.09.015.

72. Sato, T., Matsumoto, T., Kawano, H., Watanabe, T., Uematsu, Y., Sekine, K., Fukuda, T., Aihara, K.i., Krust, A., Yamada, T., et al. (2004). Brain masculinization requires androgen receptor function. Proc. Natl. Acad. Sci. USA *101*, 1673–1678. https://doi.org/10.1073/pnas.0305303101.

73. Rosenfeld, C.S. (2017). Brain sexual differentiation and requirement of SRY: why or why not? Front. Neurosci. *11*, 632. https://doi.org/10.3389/fnins.2017.00632.

74. Giudicelli, F., Gilardi-Hebenstreit, P., Mechta-Grigoriou, F., Poquet, C., and Charnay, P. (2003). Novel activities of Mafb underlie its dual role in hindbrain segmentation and regional specification. Dev. Biol. *253*, 150–162. https://doi.org/10.1006/dbio.2002.0864.

75. Inoue, S., Inoue, M., Fujimura, S., and Nishinakamura, R. (2010). A mouse line expressing Sall1-driven inducible Cre recombinase in the kidney mesenchyme. Genesis *48*, 207–212. https://doi.org/10.1002/dvg.20603.

76. Harfe, B.D., Scherz, P.J., Nissim, S., Tian, H., McMahon, A.P., and Tabin, C.J. (2004). Evidence for an expansion-based temporal Shh gradient in specifying vertebrate digit identities. Cell *118*, 517–528. https://doi.org/10.1016/j.cell.2004.07.024.

77. Winuthayanon, W., Hewitt, S.C., Orvis, G.D., Behringer, R.R., and Korach, K.S. (2010). Uterine epithelial estrogen receptor α is dispensable for proliferation but essential for complete biological and biochemical responses. Proc. Natl. Acad. Sci. USA *107*,

19272–19277. https://doi.org/10.1073/pnas.1013226107.

78. Moriguchi, T., Hamada, M., Morito, N., Terunuma, T., Hasegawa, K., Zhang, C., Yokomizo, T., Esaki, R., Kuroda, E., Yoh, K., et al. (2006). MafB is essential for renal development and F4/80 expression in macrophages. Mol. Cell Biol. *26*, 5715–5727. https://doi.org/10.1128/MCB.00001-06.

79. Tran, M.T.N., Hamada, M., Nakamura, M., Jeon, H., Kamei, R., Tsunakawa, Y., Kulathunga, K., Lin, Y.Y., Fujisawa, K., Kudo, T., and Takahashi, S. (2016). MafB deficiency accelerates the development of obesity in mice. FEBS Open Bio. *6*, 540–547. https://doi.org/10.1002/2211-5463.12058.

80. Schneider, C.A., Rasband, W.S., and Eliceiri, K.W. (2012). NIH Image to ImageJ: 25 years of image analysis. Nat. Methods *9*, 671–675. https://doi.org/10.1038/nmeth.2089.

81. Komeya, M., Yamanaka, H., Sanjo, H., Yao, M., Nakamura, H., Kimura, H., Fujii, T., Sato, T., and Ogawa, T. (2019). In vitro spermatogenesis in two-dimensionally spread mouse testis tissues. Reprod. Med. Biol. *18*, 362–369. https://doi.org/10.1002/rmb2.12291.

STAR★METHODS

KEY RESOURCES TABLE

REAGENT or RESOURCE	SOURCE	IDENTIFIER
Antibodies		
Anti Type VI Collagen (raised against cow) pAb (Rabbit, Antiserum)	Cosmo Bio Ltd.	Cat. No.: LSL-LB-1697; RRID:AB_10708895
Anti-Fibronectin antibody produced in rabbit	Sigma	Cat. No.: F3648; RRID:AB_476976
Mouse Anti-Vinculin Monoclonal Antibody, Unconjugated, Clone hVIN-1	Abcam	Cat. No.: ab11194; RRID:AB_297835
Anti-Integrin alpha 5 antibody [EPR7854] ab150361	Abcam	Cat. No.: ab150361; RRID:AB_2631309
Myosin light chain (phospho S20) antibody	Abcam	Cat. No.: ab2480; RRID:AB_303094
Phospho-FAK (Tyr397) Recombinant Rabbit Monoclonal Antibody (31H5L17)	Thermo Fisher Scientific	Cat. No.: 700255' RRID:AB_2532307
Anti human SALL1 mouse monoclonal antibody	Perseus Proteomics	Cat. No.: PP-K9814-00; RRID:AB_1964373
Anti-mouse GFP	Roche	Cat. No.: 11814460001, RRID:AB_390913
Alexa Fluor546	Molecular Probes Oregon	Cat. No.: A-11010, RRID:AB_2534077
Alexa Fluor488	Molecular Probes Oregon	Cat. No.: A-21121, RRID:AB_2535764
Alexa Fluor647	Abcam	Cat. No.: ab150079, RRID:AB_2722623
Rabbit Anti-Murine MafB Polyclonal, Unconjugated antibody	Novus	Cat. No.: NB 600-266; RRID:AB_525413
Hoechst33342	Sigma-Aldrich	Cat. No.: 875756-97-1
MafB (P-20) antibody, Santa Cruz Biotechnology	Santa Cruz Biotechnology	Cat. No.: sc-10022; RRID:AB_648633
Monoclonal ANTI-FLAG® M2 antibody	Sigma-Aldrich	Cat. No.: F1804; RRID:AB_262044
MMP-11 antibody	Abcam	Cat. No.: 1881-1, RRID:AB_765032
Chemicals, peptides, and recombinant proteins		
Tamoxifen	Sigma-Aldrich	Cat. No.: T5648
Testosterone proprionate	Sigma-Aldrich	Cat. No.: T1875
Fibronectin	Sigma	Cat. No.: F1141
Collagen VI, Human	Corning	Cat. No.: 354261
Signal Enhancer HIKARI for Western Blotting and ELISA	Nacalai Tesque	Cat. No.: 02267-41, 02270-81
Chemi-Lumi One L	Nacalai Tesque	Cat. No.: 07880-70
Critical commercial assays		
Vector TrueVIEW Autofluorescence Quenching Kit	Vector Laboratories	Cat. No.: SP-8400
Multi Tissue Dissociation Kit 1	Miltenyl Biotec Inc.	Cat. No.: 130-110-201
QIAquick PCR Purification kit	Qiagen	Cat. No.: 28104
Deposited data		
RNA sequencing data	Kajioka et al., 2021[46]	GEO: GSE158279
RNA sequencing data	This paper	GEO: GSE185966
Experimental models: Cell lines		
Human: HEK293 cells	ATCC	CRL-1573; RRID:CVCL_0045
Experimental models: Organisms/strains		
Mouse: Sall1$^{cre/+}$	Inoue et al., 2010[75]	N/A
Mouse: Shh $^{cre/+}$	Harfe et al., 2004[76]	N/A
Mouse: Wnt7a $^{cre/+}$	Winuthayanon et al., 2010[77]	N/A

(*Continued on next page*)

Continued		
REAGENT or RESOURCE	SOURCE	IDENTIFIER
Mouse: *MafB*$^{GFP/+}$	Moriguchi et al. 2006[78]	N/A
Mouse: *MafB*$^{f/f}$	Tran et al., 2016[79]	N/A
Oligonucleotides		
RNA probe: *Mmp11*	Lefebvre et al., 1992[14]	
RNA probe: *FN*	This paper	
Primer: *Mmp11* (Table S2)	This paper	
Primer: *Mmp2* (Table S2)	This paper	
Primer: *Mmp14* (Table S2)	This paper	
Recombinant DNA		
Mmp11 (NM_008606) Mouse Tagged ORF Clone	OriGene	Cat. No.: MR207900
Software and algorithms		
CellSense Standard v1.6	Olympus	
ZEN 2012 SP1 v8.1 (black edition)	Carl Zeiss	
ImageJ	Schneider et al., 2012[80]	https://imagej.nih.gov/ij/
Other		
HistoVTOne	Nacalai Tesque Inc.	Cat. No.: 06380-05
Polydimethylsiloxane (PDMS) sheets	Takehiko Ogawa; Komeya et al., 2019[81]	

RESOURCE AVAILABILITY

Lead contact

Further information and requests for reagents and resources should be directed to and will be fulfilled by the lead contact, Gen Yamada (genyama77@yahoo.co.jp).

Materials availability statement

This study did not generate new unique reagents.

Data availability statement

RNA-seq data have been deposited at GEO (GEO: GSE185966) and are publicly available as of the date of publication.

EXPERIMENTAL MODEL AND SUBJECT DETAILS

All laboratory animals were maintained under standard conditions in accordance to the Animal Use and Care Guidelines of the Wakayama Medical University, Japan. The following mouse lines were used in this study: *Shh*$^{Cre/+}$,[76] *Wnt7a*$^{Cre/+}$,[77] *Sall1*$^{Cre/+}$,[75] *MafB*$^{f/f}$,[79] and *MafB*$^{GFP/+}$.[78] All lines were on a C57BL/6J genetic background. Mice were bred, and the presence of a vaginal plug was designated as E0.5. For conditional knock-out mice, the *flox* allele was deleted by oral administration of Tamoxifen (200 mg/kg body weight) on E11.5 for *Sall1*$^{Cre/+}$*MafB*$^{f/f}$ and E9.5 for *Shh*$^{Cre/+}$*MafB*$^{f/f}$. Heterozygous or wild-type littermates were used as control. To analyze the sexual dimorphism of mRNA and protein expressions in the eExG, ICR mice were utilized. TP was orally administered at E14.5 and E15.5 at 100 mg/kg body weight to induce masculinization in female mice prior to harvest.

METHOD DETAILS

Histological analyses and imaging

All tissue samples were fixed in 4% wt/vol paraformaldehyde in PBS (PFA/PBS) and serially dehydrated in methanol. The samples were paraffin-embedded and cut into 6 μm sections for immunofluorescence and hematoxylin/eosin (HE) staining, while a thickness of 10 μm was used for mRNA *in situ* hybridization. HE

staining was performed using standard protocol. For mRNA *in situ* hybridization, the samples were deparaffinized, rehydrated, and then incubated in 65°C overnight with the mRNA probe for either *Mmp11*[14] and *FN* (forward: 5′-GCATCAGCCCGGATGTTAGA-3′; reverse: 5′-GGTTGGTGATGAAGGGGGTC-3′). The slides were then washed with 1X TBST and labeled with an anti-DIG probe (1:1000) prior to colorization with NBT/BCIP.

Proteins were detected using standard immunofluorescence protocol: the samples were deparaffinized and rehydrated before being subjected to antigen retrieval. HistoVTOne (105°C, 15 min) was used as the antigen retrieval agent for all antibodies except for anti-fibronectin (FN; 5% w/v trypsin, 5 min). For detecting extracellular matrix proteins, rabbit monoclonal antibodies for Collagen VI (ColVI; 1:1000) and FN (1:200) were used in this study. For detecting focal adhesions and related proteins, we used mouse monoclonal antibody for vinculin (VCL) (1:800) and rabbit monoclonal antibodies for integrin α5 (ITGa5; 1:200), phosphorylated focal adhesion kinase (pFAK; 1:500), and phosphorylated myosin light chain (pMLC; 1:1000). We also used the following antibodies as markers for our regions of interest: rabbit monoclonal antibody for MAFB (1:1000), mouse monoclonal antibody for SALL1 (1:200), and GFP (1:200). To reduce autofluorescence by red blood cells, slides were incubated for 5 min in TrueVIEW Autofluorescence Quenching Kit. Immunostaining was visualized using Alexa Fluor 488, Alexa Fluor 546, and Alexa Flour 647 (1:200). Nuclei was marked using Hoechst33342 (1:1000).

For immunocytochemical staining, cells were fixed in 4% PFA/PBS for 10 min, washed with PBS and permeabilized with 0.5% Triton X-. Slides were then incubated with the monoclonal antibodies targeting VCL (1:1000) and pMLC (1:1000). The cells were fluorescently labeled at a 1:300 dilution and counterstained with Hoechst 33,342 (1:2000) prior to visualization.

All sections were viewed using an Olympus BX51 microscope and processed with Cell Sans Standard (v1.6, Olympus). Confocal fluorescence images were taken using the ZEISS LSM 900 with Airyscan 2 (Carl Zeiss). The images then were processed using the ZEN 2012 SP1 v8.1 software (black edition, Carl Zeiss). Live imaging videos were taken using ZEISS LSM 900 with Airyscan 2 equipped with an incubation chamber under 5% CO2 and 37°C.

Chromatin immunoprecipitation (ChIP) assay and ChIP-Seq analysis

The proximal and ventral portions of 30 eExG samples were dissected from E16.5 male ICR mice and homogenized in lysis buffer containing 10 mM HEPES-KOH (pH 7.3), 10 mM KCl, 5 mM $MgCl_2$, 0.5 mM dithiothreitol, 0.2 mM phenylmethylsulfonyl fluoride, and protease inhibitor cocktail. The chromatin was cross-linked for 30 min with 2 mM ethylene glycol bis(succinimidyl succinate) (EGS) (Thermo Fisher Scientific, Inc) then with 1% formaldehyde for 5 min at RT. The resulting chromatin was digested using MNase (Takara) prior to being sonicated in SDS lysis buffer (50 mM Tris-HCl [pH8.1], 10 mM EDTA, 1%SDS). For the antibody reaction, 50 μg of DNA was immunoprecipitated with a specific antibody for MAFB (2.0 μg) at 4°C overnight. The immunoprecipitation buffer constituted of 16.7 mM Tris-HCl (pH8.1), 1.2 mM EDTA, 1.1% Triton X-, 0.01% SDS, 167 mM NaCl, 0.2 mM PMSF, and protease inhibitor cocktail. Dynabeads with Protein G (Life Technologies) were added to isolate protein-DNA complexes. Cross-linking was reversed at 65°C for 8 h. DNA fragments were purified by a QIAquick PCR Purification kit (QIAGEN). Polymerase chain reaction (PCR) was performed under the following conditions: 5 min at 95°C then 95°C for 10s, 55°C for 30s, 72°C for 1 min, and 72°C for 10 min for 40 cycles. The primer used for *Mmp11* is listed in Table S2. Rabbit immunoglobulin (Dako) was used as a control.

Primary cell migration assay and culture

The biMs of E15.5 male ICR embryos were dissected, and the cells were separated using the gentleMACS Octo Dissociator (Miltenyl Biotec) according to the manufacturer's instructions. Briefly, the dissected tissues were placed inside gentleMACS C tubes with 1.1 mL of serum-free DMEM and the enzyme mix provided by the manufacturer. The tissues were processed at room temperature for 30 min. The resulting single-cell suspension was precipitated and resuspended in charcoal-filtered FBS- and DHT-supplemented media. For substrate migration assay, polydimethylsiloxane (PDMS) sheets[81] were trimmed, submerged in 30 ng/cm^2 ColVI (Corning) or 30 ng/cm^2 FN (Sigma), and placed on a culture dish. The plates were incubated at 37°C for at least 20 min prior to use. Primary cells were cultured at a density of 50,000 cells and allowed to attach for 24 h before removing the PDMS sheets and imaging. For protein expression

analysis, the cells were plated at 100 cells/μL on an 8-well chamber slide coated with either 30 ng/cm^2 ColVI (Corning) or 30 ng/cm^2 FN (Sigma) for 24 h before fixation and staining. (N ≥ 3)

Mmp11 overexpression, eExG slice culture, and exogenous collagen 6 assays

HEK293 cells were thawed and cultured until confluent in DMEM supplemented with FBS and 1% penicillin-streptomycin. The cells were harvested and a MMP11-myc-DDK-tagged plasmid vector (OriGene) was electroporated into the cells. A control set-up was electroporated with a pCMV6-Entry vector. The cells were allowed to recover for 24 h in serum-free DMEM, then cultured in 10% charcoal FBS-supplemented DMEM for an additional 48 h. The conditioned media was collected and used as culture medium for eExG slices (described below). After 24 h of culture, the tissue slices were collected, fixed, and analyzed. The media from both set-ups were collected to confirm MMP11 overexpression using Western blotting. The proteins were separated using SDS-PAGE then blotted onto an Immobilon-P PVDF (polyvinylidene difluoride) membrane (Milipore). The membrane was blocked with 1% skim milk (BD Difco) in 1X TBST for 1 h, RT, prior to incubation with anti-FLAG antibody (1:1000) diluted in Signal Enhancer HIKARI for Western Blotting and ELISA Solution A (Nacalai Tesque) at 4°C, overnight. The membrane was then washed and incubated in the Signal Enhancer HIKARI Solution B (Nacalai Tesque) with HRP goat-conjugated anti-rabbit IgG (H + L) (Invitrogen) antibody. The signal was visualized using Chemi-Lumi One L (Nacalai Tesque) under the ChemiDoc XRS + system (BioRad Laboratories).

The eExG slice culture system was performed according to.[5] The eExG of E15.5 mice were dissected and embedded in 4% low-melting point agarose in PBS. The tissues were sliced to a thickness of 140 μm using a 7000smz vibratome (Campden Instruments). The Z-deflection was adjusted to 0.03 mm or lower to reduce tissue damage. For *Mmp11* overexpression assay, the slices from female eExG were placed on a Millicell Culture Insert (EMD Millipore) and cultured with either the conditioned or control media. For the exogenous ColVI assay, the slices were cultured on top of 1.5% agarose blocks that were supplemented with or without 10% ColVI (Corning), surrounded by DMEM supplemented with 10% charcoal-treated FBS, 1% penicillin-streptomycin, and 10^{-8} M DHT. The slices were kept for 24 h under 37°C and 5% CO_2 before fixation and analysis.

RNA sequencing and qPCR analysis

The biMs from the eExG of both male and female ICR mice (E13.5 and E16.5), along with the *MafB* KO and control (*MafB*$^{GFP/+}$), was collected (n ≥ 3 per group). Total RNA was isolated using ISOGEN II (Nippon Gene Co., Ltd.) and reverse transcribed with PrimeScript RT Master Mix (Perfect Real-time, Takara Bio) following the manufacturer's instructions. The preparation of the RNA libraries were entrusted to Novogene Japan K.K., and sequencing was performed using the Illumina HiSeq 4000. The data has been deposited in GEO under the accession number GSE185966. qPCR was performed using the StepOnePlus Real-Time PCR System (Applied Biosystems) with SYBR Premix Ex Taq II (TIi RNAseH Plus, Takara Bio) in triplicate. At least three biological replicates were analyzed. *GADPH* was used as internal control. Primer information is listed in Table S2.

QUANTIFICATION AND STATISTICAL ANALYSIS

qPCR data is presented as mean relative expression ±SEM Statistical significance was assessed through t-test using Microsoft Excel. A p value of less than 0.05 was considered as statistically significant difference. All experiments were performed with at least three biological replicates.